SINTECHCOM: Science, Technology and Communication Journal
Vol. 5, No. 3, June 2025, pp. 117-122, DOI: 10.59190/stc.v5i3.318

Argon plasma ionization in thermodynamic equilibrium with continuity equation

Anshori Kasri*, Saktioto, Rakhmawati Farma, Ari Sulistyo Rini, Erwin, Awitdrus
Department of Physics, Universitas Riau, Pekanbaru 28293, Indonesia

ABSTRACT

Local thermodynamic equilibrium is a foundational concept in plasma physics and heat transfer, describing a state where each small region of a system can be treated as if it is in thermodynamic equilibrium, even if the whole system is not. However, achieving accurately perfect thermodynamic equilibrium conditions in real-experiments is often challenging. It often struggles for understanding phenomena like excited states or specific Arrhenius-driven reactions. As a result, the advantages of plasma modeling with simplifications can sometimes overshadow the disadvantages of experiments. This study simulated the ionization process of argon plasma using the 4th order Runge-Kutta numerical method. The simulation, initiated with initial densities before the simulation is run, each of them is electrons 2.6×10^{18} m^{-3}, neutral argon (Ar) 2.6×10^{18} m^{-3}, positive argon ions (Ar^+) 2.6×10^{18} m^{-3}, and positive diatomic argon ions (Ar_2^+) 2.6×10^{18} m^{-3}, successfully obtained reaction rate equilibrium data at the 625th iteration. The final densities observed were 2.46×10^{18} m^{-3} for electrons, 2.27×10^{18} m^{-3} for neutral argon, 6.4×10^{15} m^{-3} for Ar^+, and 4.34×10^{17} m^{-3} for Ar_2^+. These results show the equilibrium reaction rate in argon plasma which provides information that density of electron and Ar^+ species show a decreasing trend while density of Ar and Ar_2^+ species shows an increasing trend which are the result of ionization and recombination processes in the entire plasma system.

ARTICLE INFO

Article history:

Received Apr 8, 2025
Revised May 13, 2025
Accepted Jun 26, 2025

Keywords:

Argon
Continuity
Density
Equilibrium
Plasma

* **Corresponding Author**
E-mail address: anshori.kasri7694@grad.unri.ac.id

1. INTRODUCTION

Plasma is an interesting phenomenon especially in the applied fields in various industrial and environmental applications [1-4]. At the same time, computational capabilities and numerical methods have developed rapidly to open up the possibility of new plasma information, especially complementing the model. Efforts to obtain a plasma model that is closer to the actual conditions, implemented time integration in the Runge-Kutta numerical method [5]. The main idea is to combine several procedures between plasma models.

Several studies have conducted plasma simulation studies, such as numerical modeling of plasma jets [6, 7], dielectric barrier modeling for plasma [8], plasma simulation [9], low-pressure kinetic plasma simulation [10], numerical solution of the impact of electron sparks on plasma [11], two-dimensional numerical simulation of electron spark plasma [12], electron transport simulation [13], numerical simulation of plasma in cold air [14] and others. The study used argon as a sample (or one of its samples) for plasma modeling. Argon is an attractive choice as a base gas for plasma because argon is quite good in stability [15], reproducibility [16] industrial significance, ease of producing large volume plasma [17], high efficiency, non-toxic residues [18] and cost effectiveness [19, 20] which are the basis for choosing Argon in many plasma applications. Research using numerical methods for argon plasma has also been carried out for in-depth exploration of the continuity of argon density [21] and the completion of research like this is possible to be carried out with a numerical approach whose operations are run through software [22].

2. RESEARCH METHODS

2.1. Argon Collision

Identification and determination of argon reactions obtained when conducting a literature study based on the availability of reaction rate coefficient data (A, B, and C) in the Arrhenius equation published by reference researchers, with A coefficient represents the effective frequency of successful collisions between reactant molecules (cross section) [3], B coefficient indicates how the temperature dependency of the rate constant, and C coefficient similar to activation energy, the parameter that describes the energy barrier that must be overcome for the reaction to proceed. The parameters of the Arrhenius equation are important for understanding how the rate of Argon reactions takes place.

Table 1. Argon plasma ionization and recombination reaction data.

Reaction	A (m^3/s)	B	C (K)	References
$e + Ar \rightarrow 2e + Ar^+$	2.3×10^{-14}	0.59	202,373	[23]
$2e + Ar^+ \rightarrow e + Ar$	3.17×10^{9}	-4.5	0	[24]
$Ar + Ar \rightarrow e + Ar + Ar^+$	75.97	1.5	135,300	[24]
$e + Ar + Ar^+ \rightarrow Ar + Ar$	12.6	0	-47,800	[24]
$Ar + Ar + Ar^+ \rightarrow Ar + Ar_2^+$	2.5×10^{-43}	0	0	[25]
$Ar + Ar_2^+ \rightarrow Ar + Ar + Ar^+$	5.22×10^{-16}	1	15,131	[25]
$e + Ar_2^+ \rightarrow e + Ar + Ar^+$	1.11×10^{-12}	0	34,115	[25]

The Arrhenius constant of the Argon reaction is used for the simulation. The program functions in visualizing the density of Argon changes during the reaction. Simulation or modelling of the study will observe how the density of the Argon species changes. Reaction data and several physical parameters that have been set at the limits of the research problem are used as constant values and as reaction rate parameters.

The initial stage involves a comprehensive literature review covering relevant scientific databases on argon reactions. Precise determination of specific argon reactions identifying all ionization, excitation, recombination, and other important chemical or physical processes involving argon atoms, ions, and electrons in the plasma environment. Development of computational scripts, i.e., translating the defined reaction mechanisms and associated governing equations (e.g., rate equations, transport equations) into a programmable format used for numerical simulations, including the algorithms and data structures required to process input parameters, define the system, and perform calculations required for plasma density integration. The core computational stage initiates the entire simulation. The output of this step is the temporal and/or spatial changes in plasma density, which provide quantitative data for subsequent analysis. Based on this comprehensive analysis, scientific conclusions are drawn regarding the behavior of argon plasma under the studied conditions, contributing to a deeper understanding of the underlying physical and chemical phenomena.

3. RESULTS AND DISCUSSIONS

This Argon plasma modeling involves the reaction of species, namely electrons, neutral Argon (Ar), positive Argon ions (Ar^+), and positive diatomic Argon ions (Ar_2^+). The initial input data for the argon plasma simulation run with initial values for each species. For electrons (e), the initial density was set to 2.66×10^{18} m^{-3} and a temperature of 3 eV. Electrons with sufficiently high temperatures will significantly make collisions between species easier to occur so that heavy particles will experience excitation, ionization, and so on [26]. Meanwhile, the neutral argon species (Ar) had an initial density of 2.66×10^{16} m^{-3} and a temperature of 0.2 eV. Similarly, the single argon ion species (Ar^+) and the diatomic argon ion species (Ar_2^+) both had densities of 2.66×10^{17} m^{-3} and a temperature of 0.2 eV. The Arrhenius parameter is one of the factors that influences the species density value depending on temperature [27] and after the program is finished running, the final density results are obtained as shown in Table 2.

Tabel 2. Density of argon after reaction.

Parameter	e	Ar	Ar^+	Ar_2^+
Density (m^{-3})	2.46×10^{18}	2.27×10^{18}	6.4×10^{15}	4.34×10^{17}
Density logarithm (m^{-3})	$10^{18.3812}$	$10^{18.3569}$	$10^{15.8061}$	$10^{17.6379}$

This modeling also produces a graph of the density changes of each Argon plasma species to achieve thermodynamic equilibrium, as presented in Figure 1.

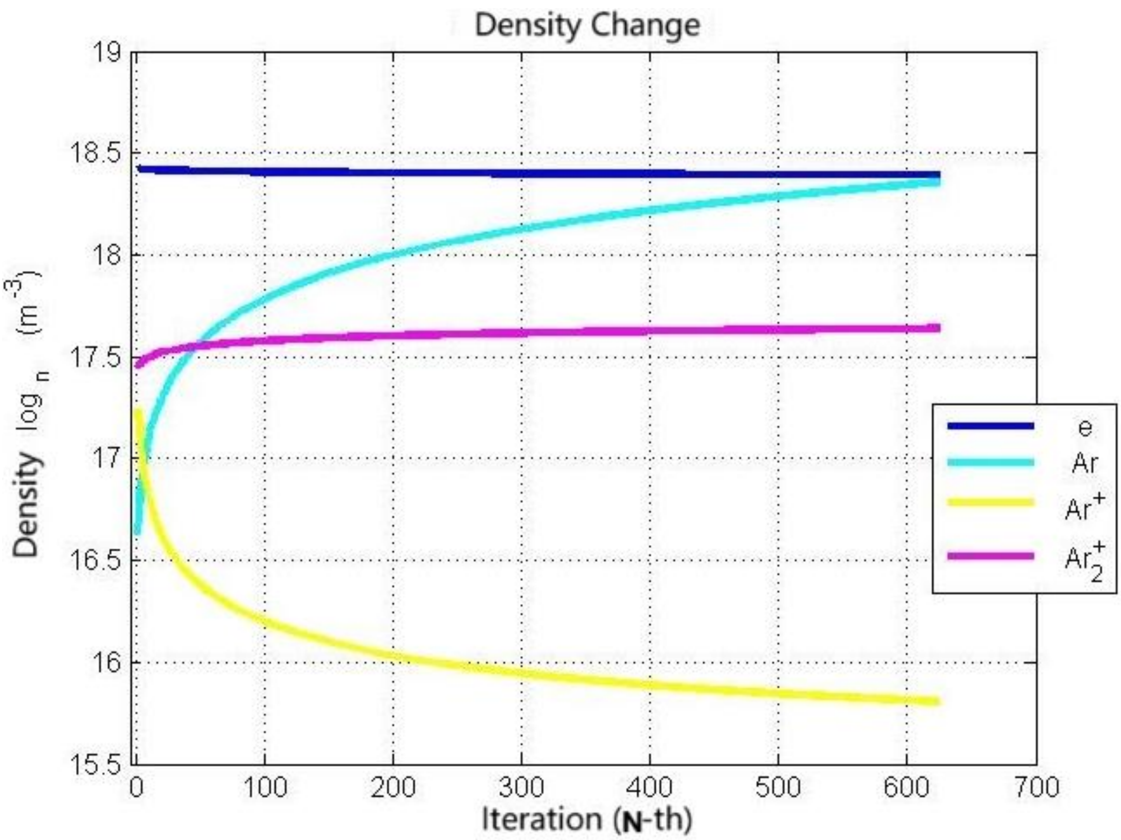

Figure 1. Density changes of argon plasma species.

The density of Ar species in Figure 1 shows an increase which means that there is a recombination process and this is in accordance with the results obtained by Zakky et al. (2023) [21]. The Ar^+ species decreased while the Ar_2^+ species increased although less than the Ar^+ species. This happens because after the collision in the reactions in the plasma, some of the Ar^+ species undergo a series of processes which eventually form into Ar_2^+ species at equilibrium and also recombine into Ar species. Electron species generally do not experience many changes compared to the Ar^+ species which appear significant because in the overall reaction there is more restructuring of Ar^+ to Ar_2^+.

Figure 2, it can also be seen that the electron density graph shows a decreasing trend that has the same pattern as the results of the research by Zakky et al. (2023) whose electron density decreased throughout the reaction process until it finally reached equilibrium as indicated at the end of the species graph showing a flat trend indicating that equilibrium has been reached [21]. Figure 3 shows the amount of density throughout the iteration. This modeling seeks the equilibrium density of the argon species until the 625th iteration with the largest reaction rate of 7.75×10^2 m^3/s and the smallest reaction rate value of 5.95×10^{-18} m^3/s.

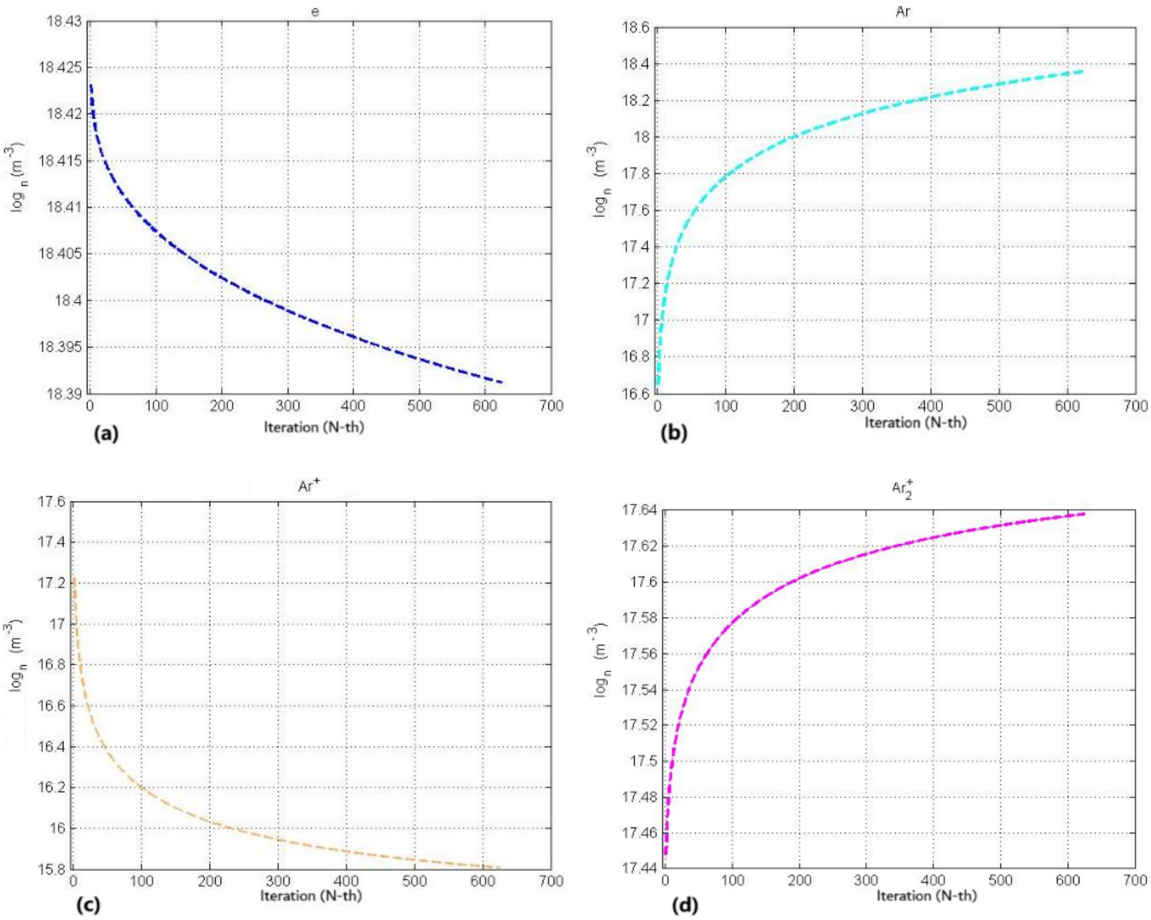

Figure 2. Changes in density of (a) electrons, (b) Ar, (c) Ar^+, and (d) Ar_2^+.

4. CONCLUSION

The research has been successfully conducted and conclusions have been obtained. The conclusions obtained include that in plasma equilibrium conditions, the density of each species shows significant differences. The electron density (e) was recorded as the highest with a value of 2.46×10^{18} m^{-3}, followed by neutral argon atoms (Ar) with a density of 2.27×10^{18} m^{-3}. The density of single argon ions (Ar^+) is much lower, which is 6.4×10^{15} m^{-3}, while molecular argon ions (Ar_2^+) have an intermediate density of 4.34×10^{17} m^{-3}. This indicates that in equilibrium conditions, the population of electrons and neutral argon atoms dominate the plasma, while the formation of molecular ions is also significant although not as much as neutral species and electrons. Single argon ions are present in relatively small concentrations. Analysis of the reaction rates that occur in argon plasma shows a very wide range of values. The largest reaction rate recorded was 7.75×10^2 m^3/s and the smallest reaction rate was 5.95×10^{-18} m^3/s and the species in the argon plasma reached equilibrium at the 625th iteration. For further work to involve various argon species in larger quantities of spesies so that the observation simulation becomes broader.

ACKNOWLEDGEMENTS

The authors would like to thank the Department of Physics and the Laboratory of Plasma and Computational Physics, Universitas Riau for the support and provision of laboratory facilities used in this research.

REFERENCES

[1] Samal, S. (2017). Thermal plasma technology: The prospective future in material processing. *Journal of cleaner production*, **142**, 3131–3150.

[2] Zhou, Y., Zhu, L., Yang, B., Fan, L., Meng, X., Chu, R., Jiang, X., Li, P., Li, W., & Chen, H. (2024). Heavy metal migration regimes in the production of syngas from solid waste by thermal plasma treatment. *Journal of Hazardous Materials*, **461**, 132698.

[3] Ipkawati, N. & Saktioto. (2019). Penentuan densitas plasma hidrogen nontermal pada tekanan rendah. *Komunikasi Fisika Indonesia*, **16**(1), 29–34.

[4] Alifah, S. N. & Saktioto. (2019). Kebergantungan temperatur plasma hidrogen dalam tekanan rendah. *Komunikasi Fisika Indonesia*, **16**(2), 118–122.

[5] Ho, A., Datta, I. A. M., & Shumlak, U. (2018). Physics-based-adaptive plasma model for high-fidelity numerical simulations. *Frontiers in Physics*, **6**, 105.

[6] Ouali, M. & Lagmich, Y. (2024). Modeling and numerical simulation of argon based DBD plasma jets: Mathematical approaches and local energy approximation. *2024 International Conference on Computing, Internet of Things and Microwave Systems (ICCIMS)*, 1–5.

[7] Barkaoui, G., Halima, A. B., Jomaa, N., Charrada, K., & Yousfi, M. (2021). A numerical simulation of a low-temperature argon plasma jet. *IEEE Transactions on Plasma Science*, **49**(4), 1302–1310.

[8] Van Laer, K. & Bogaerts, A. (2015). Fluid modelling of a packed bed dielectric barrier discharge plasma reactor. *Plasma Sources Science and Technology*, **25**(1), 015002.

[9] Sala, M., Tonello, E., Uccello, A., Bonnin, X., Ricci, D., Dellasega, D., Granucci, G., & Passoni, M. (2020). Simulations of argon plasmas in the linear plasma device GyM with the SOLPS-ITER code. *Plasma Physics and Controlled Fusion*, **62**(5), 055005.

[10] Halima, A. B., Hajji, S., Barkaoui, G., Charrada, K., & Zissis, G. (2018). Numerical simulation of plasma kinetics in a low-pressure inductively coupled discharge in argon and mercury mixtures. *IEEE Transactions on Plasma Science*, **47**(1), 162–172.

[11] Zheltukhin, V. & Chebakova, V. (2017). Numerical solution of the model problem of CCRF-discharge at atmospheric pressure. *MATEC Web of Conferences*, **129**, 03017.

[12] Bai, X., Chen, C., Li, H., & Liu, W. (2017). Two-dimensional numerical simulation of a continuous needle-like argon electron-beam plasma. *Physics of Plasmas*, **24**(5).

[13] Rabie, M. & Franck, C. (2016). METHES: A Monte Carlo collision code for the simulation of electron transport in low temperature plasmas. *Comput. Phys. Commun.*, **203**, 268–277.

[14] Chang, C. H. & Ramshaw, J. D. (1993). Numerical simulations of argon plasma jets flowing into cold air. *Plasma Chemistry and Plasma Processing*, **13**, 189–209.

[15] Shi, J. J., & Kong, M. G. (2007). Radio-frequency dielectric-barrier glow discharges in atmospheric argon. *Applied Physics Letters*, **90**(11).

[16] Golda, J., Held, J., & Schulz-von der Gathen, V. (2020). Comparison of electron heating and energy loss mechanisms in an RF plasma jet operated in argon and helium. *Plasma Sources Science and Technology*, **29**(2), 025014.

[17] Moon, S. Y., Han, J., & Choe, W. (2006). Control of radio-frequency atmospheric pressure argon plasma characteristics by helium gas mixing. *Physics of Plasmas*, **13**(1).

[18] Mohamed, A. J., Khalaf, M. K., & sabir Jasim, A. (2022). The study of the characteristics of a microwave plasma jet operated with Ar at atmospheric pressure. *Tikrit Journal of Pure Science*, **27**(4), 70–76.

[19] Yunata, E. E. & Ghufron, M. (2020). The study of argon plasma based on experimental and modeling diagnosis. *AIP Conference Proceedings*, **2314**(1).

[20] Xia, W., Liu, D., Xu, H., Wang, X., Liu, Z., Rong, M., & Kong, M. G. (2018). The effect of ethanol gas impurity on the discharge mode and discharge products of argon plasma jet at atmospheric pressure. *Plasma Sources Science and Technology*, **27**(5), 055001.

[21] Zakky, F., Fardinata, R., & Abd Aziz, M. S. (2023). Equilibrium of argon plasma particles at high pressure. *Science, Technology and Communication Journal*, **4**(1), 23–32.

[22] Rodriguez, I. J. (2018). *Some Assembly Required: computational simulations of dusty plasma*. Magister Thesis, Portland State University.

[23] Gudmundsson, J. T. & Thorsteinsson, E. G. (2007). Oxygen discharges diluted with argon: dissociation processes. *Plasma Sources Science and Technology*, **16**(2), 399.

[24] Baeva, M., Gorchakov, S., Kozakov, R., Uhrlandt, D., & Schoenemann, T. (2013). Non-equilibrium modelling of the electrical characteristics of a free-burning arc. *High Voltage Engineering*, **39**(9), 2159–2165.

[25] Lam, S. K., Zheng, C. E., Lo, D. Y., Dem'Yanov, A., & Napartovich, A. P. (2000). Kinetics of Ar* 2 in high-pressure pure argon. *Journal of Physics D: Applied Physics*, **33**(3), 242.
[26] Fardinata, R., Saktioto, & Farma, R. 2023. Pemodelan generator plasma hidrogen frekuensi gelombang mikro tekanan atmosfir. *Komunikasi Fisika Indonesia*, **20**(3), 205–214.
[27] Devira, N. & Saktioto. 2022. Penggunaan pemodelan sumber plasma helium pada keadaan setimbang untuk aplikasi plak gigi. *Komunikasi Fisika Indonesia*, **19**(1), 11–18.